NANO LETTERS

2007
Vol. 7, No. 11
3366−3371

Room-Temperature Ferromagnetism in Cu Doped GaN Nanowires

Han-Kyu Seong,[†] Jae-Young Kim,[*,‡] Ju-Jin Kim,[§] Seung-Cheol Lee,[||] So-Ra Kim,[§] Ungkil Kim,[†] Tae-Eon Park,[†] and Heon-Jin Choi[*,†]

Department of Materials Science and Engineering, Yonsei University, Seoul 120-749, Korea, Pohang Accelerator Laboratory & Department of Physics, Pohang University of Science and Technology, Pohang 790-784, Korea, Department of Physics, Chonbuk National University, Jeonju 561-756, Korea, and Future Technology Research Division, Korea Institute of Science and Technology, Seoul 136-791, Korea

Received July 9, 2007; Revised Manuscript Received September 8, 2007

ABSTRACT

We report magnetism in Cu doped single-crystalline GaN nanowires. The typical diameter and the length of the $Ga_{1-x}Cu_xN$ nanowires ($x = 0.01, 0.024$) are 10−100 nm and tens of micrometers, respectively. The saturation magnetic moments are measured to be higher than 0.86 μ_B/Cu at 300 K, and the Curie temperatures are far above room temperature. Anomalous X-ray scattering and X-ray diffraction measurement make it clear that Cu atoms substitute the Ga sites, and they largely take part in the wurtzite network of host GaN. X-ray absorption and X-ray magnetic circular dichroism spectra at Cu $L_{2,3}$ edges show that doped Cu has local magnetic moment and the electronic configuration of it is mainly $3d^9$ but mixed with a small portion of trivalent component. It seems that the ionocovalent bonding nature of Cu 3d orbital with surrounding semiconductor medium makes Cu atom a mixed electron configuration and local magnetic moments. These outcomes suggest that the $Ga_{1-x}Cu_xN$ system is a room-temperature ferromagnetic semiconductor.

The concept of simultaneously manipulating both charge and spin in a single-semiconductor medium leads to the exciting area of spintronics.[1,2] Semiconductors doped with transition metal, so-called diluted magnetic semiconductors (DMSs), are the most promising candidates for such applications.[3,4] According to the principle of mean field theory,[3] transition metals such as Sc, Ti, V, Cr, Mn, Fe, Co, and Ni that have partially filled d states can be doped for transforming spin-frustrated semiconductors to ferromagnets. It has also been predicted that room-temperature ferromagnetism, which would be advantageous in many applications, could be achieved in magnetic doped wide band gap semiconductors.[5] Indeed, room-temperature ferromagnetism has been reported from Cr, Mn, Fe, and Co doped GaN, ZnO, and TiO_2.[6−8] However, these transition metals with local magnetic moments may not be the best choice for the doping elements. Magnetic secondary clusters have been shown to be ferromagnetic, arguing the motivation that the ferromagnetism of the DMSs arises from magnetic secondary clusters.[9−11] Namely, the origin of ferromagnetism in these DMSs is still controversial due to the possibility of magnetic secondary phases and uncertainty of magnetic interactions.

In the present study, we utilize a $Ga_{1-x}Cu_xN$ nanowire system. Cu is a *nonmagnetic* element. However, if it is doped into a semiconductor as divalent states, the partially filled d states of Cu^{+2} ions render it a candidate for achieving ferromagnetism. Importantly, if ferromagnetism is realized, there will be no need to consider the contribution of controversial secondary phases because no ferromagnetic compounds exist in this system. Nanowires also have a number of advantages over thin films with respect to studying ferromagnetism in DMSs. Specifically, they offer thermodynamically stable features and are typically single-crystalline and defect free. They can thus safely exclude the effect of defects and nonuniform distribution of dopants that are typically observed in DMSs prepared by nonequilibrium processing (e.g., molecular beam epitaxial process). The free-standing nature of nanowires makes it possible to exclude the effect of thermal and lattice mismatch of the substrate and opens the possibility of determining the *intrinsic* magnetism under fully relaxed states.[12] Moreover, nanowires could further fuel the development of ferromagnetism in DMSs. For example, all spin rotations in the nanowire could be limited to a single axis. In addition, the spin rotation operators commute, predicting a progressive slowing and finally a complete suppression of the spin relaxation.[13] Possible tetragonal distortion and shape anisotropy in the nanowires could also be helpful for the evolution of

* Corresponding authors. E-mail: hjc@yonsei.ac.kr H.-J.C.; masson@postech.ac.kr (J.-Y.K.).
[†] Yonsei University.
[‡] Pohang University of Science and Technology.
[§] Chonbuk National University.
[||] Korea Institute of Science and Technology.

10.1021/nl0716552 CCC: $37.00
Published on Web 09/29/2007

ferromagnetism.[14,15] Last, nanowires themselves are attractive building blocks for electronic devices. Herein, we report magnetism in Cu doped single-crystalline GaN nanowires. The cusp at the Cu *K* edge of anomalous X-ray scattering (AXS) spectra indicates that Cu atoms substitute the Ga sites and largely take part in the wurtzite network of host GaN, which is also confirmed by the Bragg peak shift of X-ray diffraction (XRD) pattern. It is clear that the doped Cu has a local magnetic moment and a mixed valence state by measuring the X-ray magnetic circular dichroism (XMCD) and X-ray absorption spectroscopy (XAS) at Cu $L_{2,3}$ edges. The room-temperature ferromagnetic $Ga_{1-x}Cu_xN$ nanowires are expected to open a pathway toward a new class of nonmagnetic doped diluted magnetic semiconductors.

Single-crystalline diluted magnetic semiconductor $Ga_{1-x}Cu_xN$ nanowires for $x = 0.01$ and 0.024 were synthesized using a Ni catalyst deposited *c*-plane sapphire substrates in a horizontal hot-wall chemical vapor transport system. Solid metallic Ga (purity 99.99%) and CuCl (purity 99.99%) powder were inserted into the center of a quartz tube at intervals of 2 in., respectively. The substrates were placed at a distance of 1 in. away from metallic Ga. The temperature of the furnace was increased at a heating rate of 50 °C min^{-1} to 800 °C under flow of NH_3 at a rate of 20 cm^3 min^{-1} and kept for 10 through 60 min and then cooled down to room temperature.

Figure 1a shows a scanning electron microscopy (SEM) image of typical nanowires grown on the substrate. The diameter and length of these nanowires are from 10 to 100 nm and tens of micrometers, respectively, and they have a triangular structure (inset in Figure 1a). The nanowires were sonicated in ethanol and deposited onto molybdenum grids for transmission electron microscopy (TEM) and energy dispersive spectroscopy (EDS) analyses. Figure 1b shows a high-resolution transmission electron microscopy (HRTEM) image. Single-crystalline nature without defects or secondary phases can be seen in all of the HRTEM images. The selected area electron diffraction (SAED) pattern recorded on the wire, as shown in Figure 1c, indicates that the nanowires grow in the $[1\bar{1}00]$ direction, perpendicular to the (1000) crystal plane. Figure 1d shows the representative Cu concentration, as determined by an energy dispersive spectroscopy (EDS) analysis. The average Cu concentration measured from ten nanowires was ca. 1% and 2.4%, respectively, depending on the processing conditions. The catalyst Ni was etched out clearly by the chloride vapors during the growth of the nanowires in our process, as proved in our earlier studies.[16,17] It was also confirmed by XAS measurements at Ni $L_{2,3}$ edges (not shown). It is well-known that the sensitivity of XAS at *L* edges on 3d transition metals is especially high because the 3d atomic orbitals are well localized. For pure Ni, the peak of XAS is 10 times higher than the background continuum and the noise level is less than 0.1% of background. Therefore, the detection limit of XAS on Ni is about 0.01%, however, we found no peak for the Ni *L* edges. The synchrotron XRD patterns of the $Ga_{1-x}Cu_xN$ nanowires were indexed to be a wurtzite structure and no detectable peaks

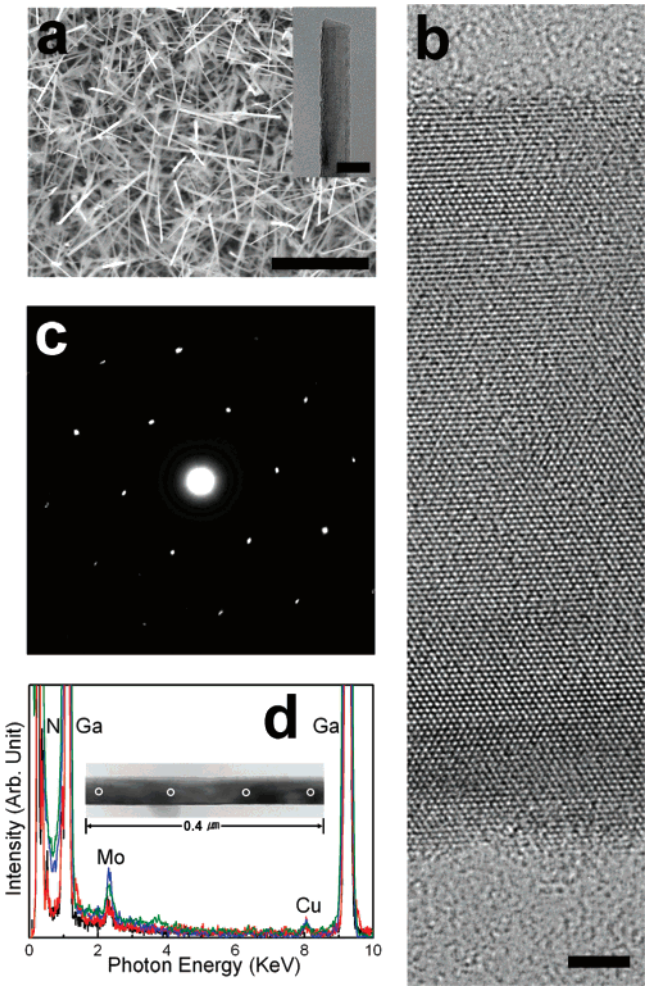

Figure 1. Synthesis and structural characterization of $Ga_{1-x}Cu_xN$ nanowires. (a) Typical SEM image of $Ga_{1-x}Cu_xN$ nanowires grown on the sapphire substrate. Inset is TEM image of the nanowire showing a triangular structure. The scale bars in (a) and inset are 5 μm and 50 nm, respectively. (b) HRTEM image of a nanowire with diameter of 50 nm. The scale bar is 2 nm. (c) SAED pattern of the nanowire, recorded on the [0001] zone axis. (d) EDS spectra collected from different positions within the $Ga_{1-x}Cu_xN$ nanowires as marked with ○. Inset is a TEM image of a nanowire. The spectra show essentially the same compositions without any evidence of phase inhomogeneity.

corresponding to any of the Cu/Ni-related secondary phases were found (Figure S1, Supporting Information).

Figure 2 shows the magnetic properties measured with a superconducting quantum interference device (SQUID) magnetometer. As shown in this figure, the $Ga_{1-x}Cu_xN$ nanowires are ferromagnetic, with a Curie point exceeding room temperature. Parts a and b of Figure 2 are the magnetization versus magnetic field (M−H) curves for $x = 0.01$ and 0.024, measured at 5 and 300 K, respectively. The hysteresis loops were obtained after appropriate correction for the diamagnetic component arising from the sapphire substrate. The magnetization increases steeply at a low field and saturates at about >2.0 KOe. A clear hysteresis loop at both temperatures was observed, although the magnetization increases with Cu concentration. The pure GaN nanowires grown on the substrate using identical process showed diamagnetic behavior (inset in Figure 2a). A magnetic moment for

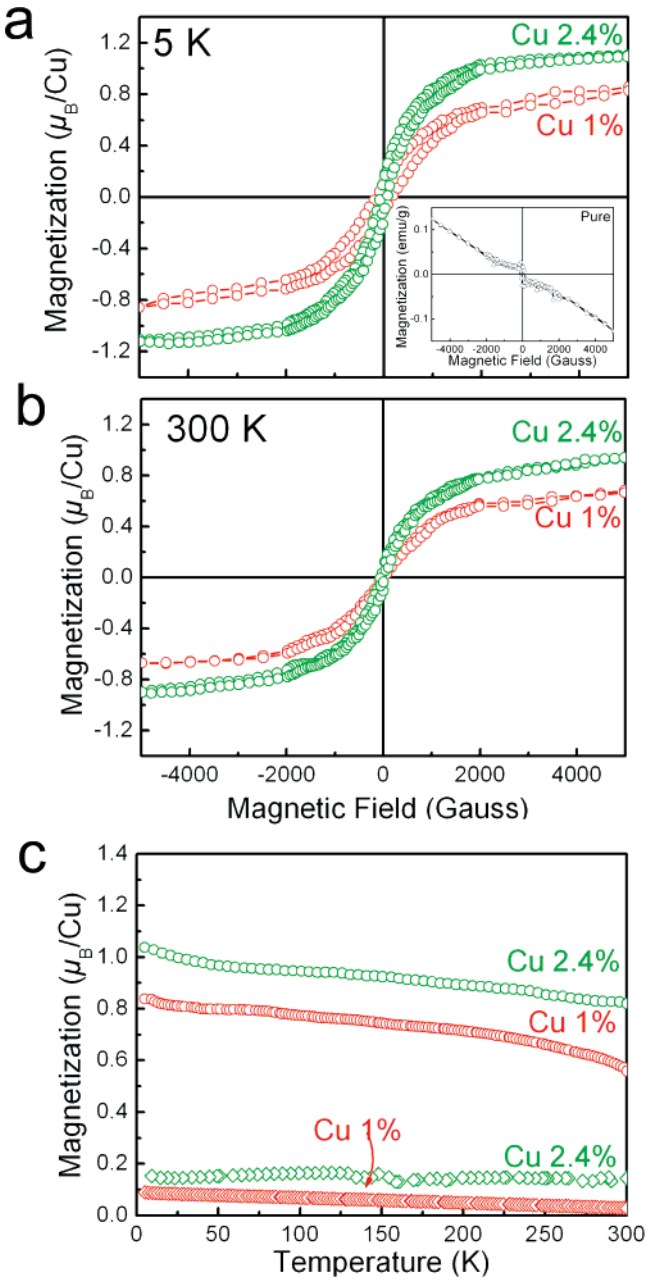

Figure 2. Magnetic properties of $Ga_{1-x}Cu_xN$ nanowires. (a,b) Magnetization vs magnetic field (M−H) of nanowires ($x = 0.01$ and 0.024) measured at 5 and 300 K, respectively. Inset shows magnetic properties of pure GaN nanowires indicating diamagnetics. (c) Temperature-dependent magnetization (M−T) of at 200 G (diamonds) and 5000 G (circles) for $Ga_{1-x}Cu_xN$ nanowires. The curves show the nonzero magnetization up to room temperature.

$Ga_{0.976}Cu_{0.024}N$ nanowires in Figure 2b is 0.86 μ_B (1 $\mu_B \times 10^{-24}$ Am^2) per Cu atom at 300 K. The temperature-dependent magnetization ($M-T$) curve further shows the nonzero magnetization up to room temperature (Figure 2c), and temperature-dependent resistance of an individual nanowire was not observed any anomalous behaviors in range of 5−300 K (Figure S2, Supporting Information).[18,19] From these measurements, it becomes clear that the ferromagnetism of $Ga_{1-x}Cu_xN$ nanowires is robust even above the room temperature.

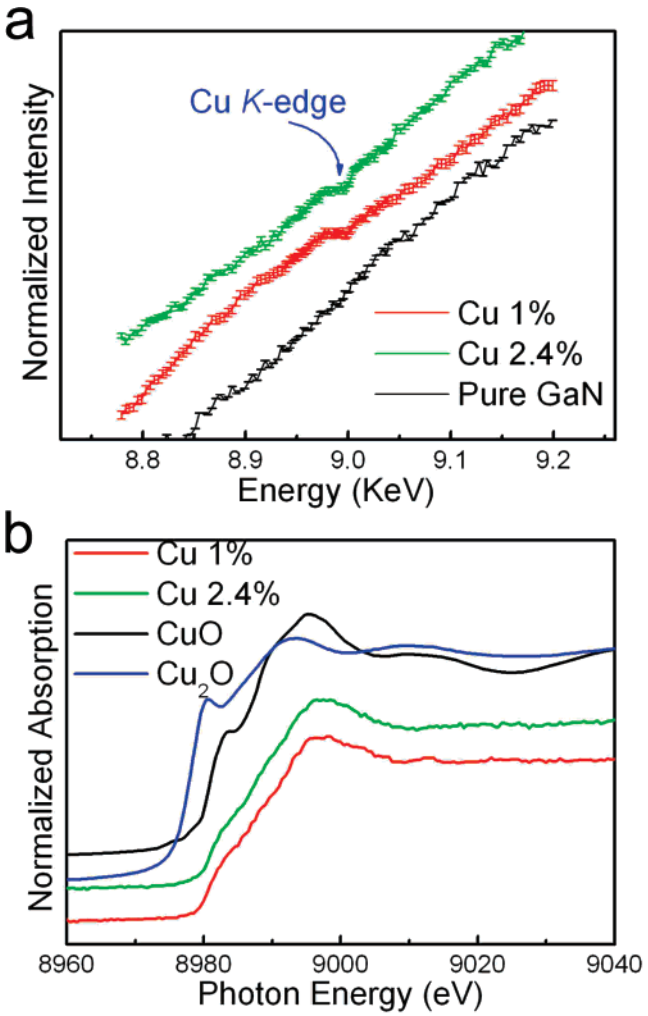

Figure 3. Structural and chemical information of $Ga_{1-x}Cu_xN$ nanowires. (a) AXS spectra of pure GaN and $Ga_{1-x}Cu_xN$ nanowires for $x = 0.01$ and 0.024 measured at the $(10\bar{1}0)$ and (0002) Bragg peak position across the K absorption edges for Cu at 8.979 keV, respectively. (b) Normalized XANES spectra of Cu in $Ga_{1-x}Cu_xN$ nanowires, Cu_2O, and CuO powders as reference samples measured at 300 K, respectively. The spectra of the nanowires well correspond to the CuO in their pre-edge regions, whereas Cu_2O denotes the pre-edge peak at 8980.4 eV.

To investigate whether Cu dopants are incorporated in the crystalline lattice of GaN nanowires or not, we measured AXS for the $Ga_{1-x}Cu_xN$ nanowires around Cu K absorption edge. AXS measurements were carried out at the beamline 5A of the Pohang Light Source (PLS). For the AXS measurements, the diffraction intensity was measured as a function of momentum transfer at incident X-ray energy and the scattering intensity was monitored as the X-ray energy was varied through the Cu K absorption edge. Good counting statistics were ensured in data collection. Figure 3 shows the AXS spectra, taken by measuring diffraction intensity as a function of photon energy while keeping the scattering vector q at the Bragg peak. The diffused fluorescence background was also measured simultaneously and subtracted. In AXS, the anomalous form factors change near the absorption edge. If the element is associated with Bragg peak, then elemental absorption causes a decrease in the

Bragg intensity at its absorption edge, and a cusp caused by the interference between the Thomson scattering amplitude and the real part of the anomalous scattering amplitude appears in the energy scan of the Bragg peak.[20] Such behavior was observed for the $Ga_{1-x}Cu_xN$ nanowires for $x = 0.01$ and 0.024. As shown in Figure 3a, Cu in the nanowires was found to be associated with the Bragg peak, showing that the spectra exhibit an intensity cusp at the Cu *K* edge. However, it is clearly absent for pure GaN. It certainly indicates that doped Cu atoms participate in the wurtzite network of host GaN. It is supported by the result from XRD measurements (Figure S1, Supporting Information). The Bragg peaks are shifted without noticeable broadening when Cu is doped. It indicates the change of lattice parameters due to the incorporation of Cu into the GaN lattice. We found that the valence count of doped Cu is primarily 2+ by measuring the Cu *K*-edge X-ray absorption near-edge spectroscopy (XANES). In Figure 3b, the spectra for Cu doped nanowires are compared with that of CuO (d^9) and Cu_2O (d^{10}), which have been measured at the same time. They are mainly the dipole transition from Cu 1s to 4p, with a small contribution of quadrupole transition from Cu 1s to 3d. The spectra for both nanowires are identical and the overall line shape is similar with that of CuO, but they are largely different from Cu_2O.[21,22] Especially the position of absorption edge has a coincidence with CuO. It indicates that the doped Cu is largely in a 2+ charge state.

To study the valence of 3d states more precisely Cu $L_{2,3}$ edges XAS were also measured because they will present the dipole transition probability from Cu 2p to Cu 3d and provide the information on the 3d states more directly than *K* edge. Figure 4a shows the *L* edge spectra for Cu doped nanowires and CuO for comparison. Cu spectra for both nanowires are identical and the largest peak locates at the same energy 931 eV with $3d^9$ ground state of CuO. And there is another smaller peak at 3.5 eV higher energy. There is no corresponding peak in divalent or monovalent Cu compounds.[23,24] It is common in XAS spectra that higher valent states of 3d transition metals appear at 2−4 eV higher energy because of reduced Coulomb energy between core hole and valence electrons of the final state. Accordingly, we expect that it is associated with trivalent state. The identical line structure is reproduced at L_2 region. Therefore it is confirmed again that the electronic configuration of doped Cu is mainly $3d^9$. The formal ionic valence of Cu at cation site of GaN is trivalent, but it seems that the locally divalent state is preferred by the covalent bonding with nitrogen, suggesting that the ionocovalent bonding nature of the Cu 3d orbital with the surrounding semiconductor medium makes Cu atom a mixed electron configuration.

If it is, the spins of the 3d orbital are not paired and the doped Cu should have local spin magnetic moment. To check whether the local spin moments align ferromagnetically or not, we also measured XMCD spectra of Cu $L_{2,3}$ absorption edges. XMCD measurements were carried out at the 2A1-EPU beamline of PLS. For the XMCD measurement, the degree of circular polarization of the incident light was set to be 95% and a 5000 G magnetic field produced by an

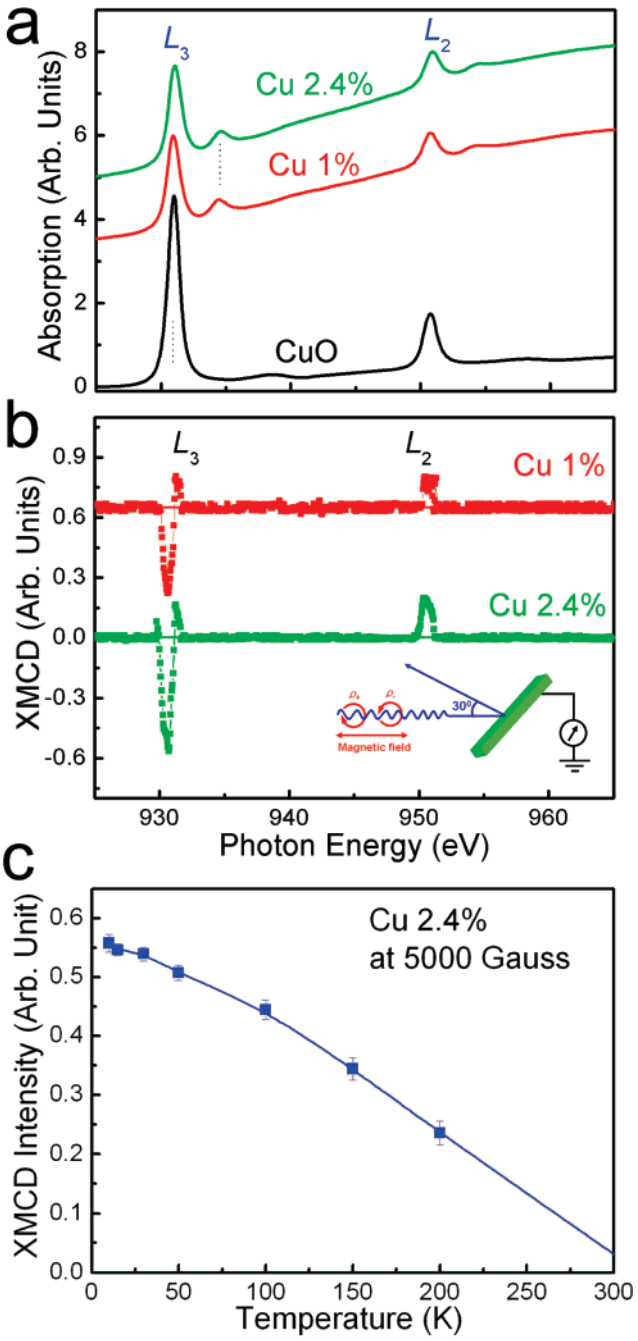

Figure 4. Ferromagnetic origin of $Ga_{1-x}Cu_xN$ nanowires for $x = 0.01$ and 0.024. (a) XAS spectra at the Cu $L_{2,3}$ edge for CuO powder and $Ga_{1-x}Cu_xN$ nanowires measured at 300 K. The spectra are largely separate into 2 regions of L_3 and L_2, which is caused by the spin orbit splitting of core level. It is well-known that the 931 eV peak of CuO corresponds to $3d^9$ ground state (from 2p to 3d dipole transition) and the other peak around 7 eV higher energy is associated with $3d^{10}$ ground states (from 2p to 4s dipole transition). (b) XMCD data ($\rho_+ - \rho_-$) from the difference between the Cu L_{23} edge XAS spectra for the different spin directions (ρ_+ and ρ_-) of nanowires measured at 10 K, which were normalized by the photon flux. Inset is measurement setup with respect to magnetic field (5000 G) at 30° relative to the surface normal. (c) Temperature dependence of the dichroism for the nanowires for $x = 0.024$.

electromagnet was applied along the surface normal of the substrate to align the spin moment. All of the spectra were obtained in a total electron yield (TEY) mode. As shown in

Figure 4b, the dichroism signal is measured successfully. Accordingly, it is proven that the doped Cu provides the local magnetic moment and it is the origin of the room-temperature ferromagnetism of $Ga_{1-x}Cu_xN$ nanowires for $x = 0.01$ and 0.024. In this system, no XMCD dichroism signals at Ni $L_{2,3}$ edge in the same samples were observed such as in the metallic or secondary phase of Ni catalyst employed in the wire fabrication process (Figure S3, Supporting Information). As shown in Figure 4c, the temperature dependence data for $x = 0.024$ reveal the ferromagnetic ordering temperature of ~300 K. A substantial tail in the dichroism persists up to the 300 K ordering temperature, in agreement with a Curie point above room-temperature seen in the temperature-dependent magnetization curve of SQUID measurements. This further suggests that the nanowires are room-temperature ferromagnetic and the induced host moments are clearly associated with the ferromagnetic phase in Cu doped GaN and argue strongly against a role of any secondary phase and impurity in the origin of ferromagnetism.

The ferromagnetic nature of the nanowires can be further confirmed by magnetoresistance (MR) measurement of individual $Ga_{1-x}Cu_xN$ nanowires. Because direct observation of magnetization in nanostructures is difficult, MR measurements on an individual nanowire can be used as a sensing tool to determine the magnetization reversal process of an individual nanowire. For MR measurements, the nanowire was prepared on an oxidized Si substrate. The patterns for electrical leads were generated via electron beam lithography onto the selected nanowire and metal electrodes (Ti/Au bilayer, 45/35 nm) were then deposited on the contact area by electron beam evaporation. Figure 5a shows an SEM image of a $Ga_{1-x}Cu_xN$ nanowire. From an individual nanowire contracted with two nonmagnetic Ti/Au electrodes to prevent influence of the contact structures on the magnetization reversal process (Figure 5a). We carried out MR measurements in a He^4 cryostat at a temperature of $T = 4.2$ K. A magnetic field up to $H = \pm 1$ T was applied to the sample in the parallel and perpendicular directions with respect to the long axis of the nanowire, respectively. As shown in parts b and c of Figure 5, the resistance curves exhibited clear hysteretic behavior with two resistance minima at the switching fields for both parallel and perpendicular directions of the applied magnetic field with respect to the wire axis, which were considered coersive fields. Different behaviors (negative and positive MR) observed for the two different magnetic fields indicate that the magnetization in the remanent state lies mostly along the axis of the $Ga_{1-x}Cu_xN$ nanowires. Furthermore, at a switching field of $H = \pm 200$ G, the resistance sharply increases in both sweeping directions. Observations of hysteretic MR and switching fields clearly demonstrate the ferromagnetism of the $Ga_{1-x}Cu_xN$ nanowires.

In summary, ferromagnetism was achieved from Cu doped wide band gap GaN semiconductor nanowires. As shown in our magnetic measurements, the Curie point of this magnetic semiconductor is much higher than room temperature. Importantly, magnetic secondary phases are not responsible for the observed room-temperature ferromagnetism because

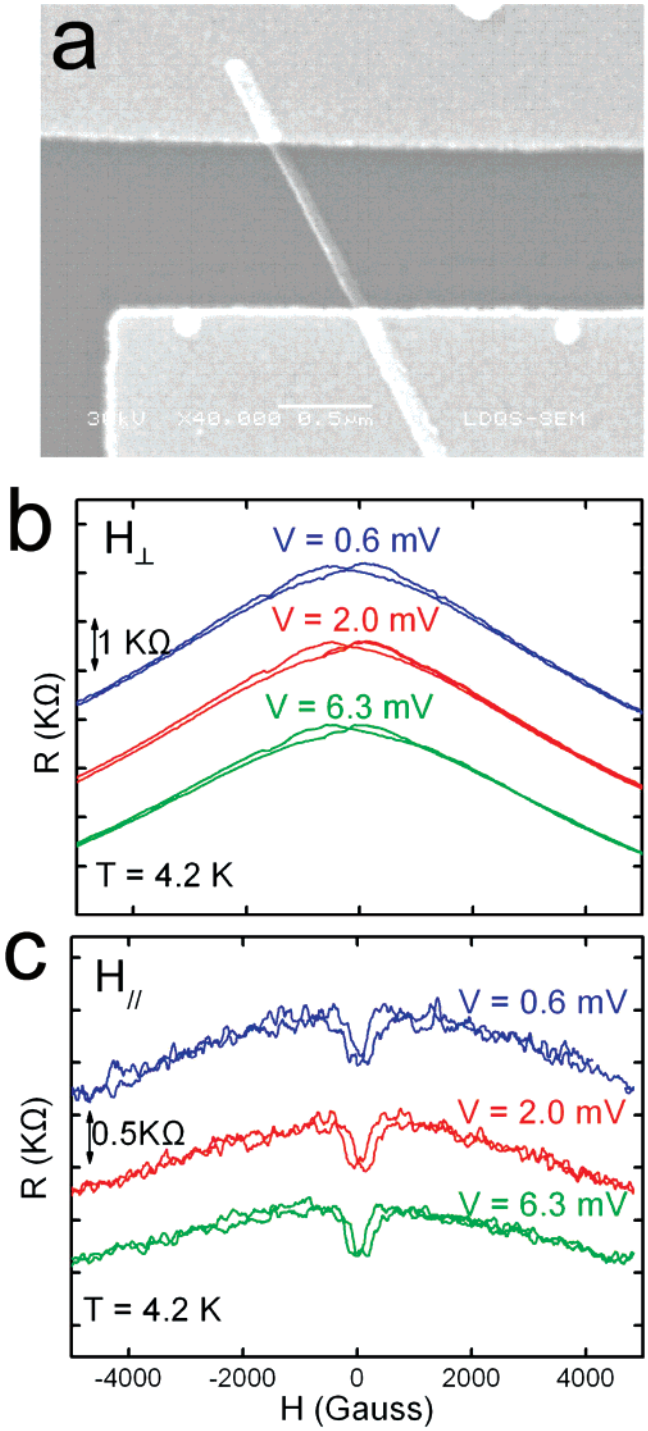

Figure 5. Current-driven spin response of a single $Ga_{1-x}Cu_xN$ nanowire measured at 4.2 K. (a) SEM image of a typical $Ga_{1-x}Cu_xN$ nanowire with two *nonmagnetic* Ti/Au electrodes. Magnetoresistance of the nanowire for $x = 0.01$ (b) and $x = 0.024$ (c) with bias voltages of 0.6, 2.0, and 6.3 mV with magnetic field applied perpendicular and parallel to the wire axis, respectively.

no such phases exist in the system. Instead, it may be attributed to p−d hybridization between Cu and N ions, which induces delocalized magnetic moments and long-range coupling. It should be noted that theoretical calculations and limited experiments involving Cu doped oxide systems (e.g., ZnO and TiO_2) have also shown room-temperature ferromagnetism.[25−29] In these systems, however, the Cu ions are

strongly localized and hybridized with oxygen 2p orbitals,[28,29] suggesting that carrier-induced ferromagnetism for manipulating the spin and charge of a single-semiconductor medium may be difficult to realize without additional doping for the carrier generation. In the Cu doped GaN system, on the contrary, Cu^{+2} ions induce long-range coupling of unpaired spins, and thus the system can be regarded as a new class of DMSs that realize room-temperature ferromagnetism by coupling between carriers and local moments of nonmagnetic spins.

Acknowledgment. This research was supported in part by a grant from the National Research Laboratory of the Korean Ministry of Science and Technology, the Korea Research Foundation (MOEHRD, KRF-2005-042-D00203), and the Second Stage of Brain Korea 21 Project in 2007. J.-J.K. acknowledges the support from the Electron Spin Science Center at POSTECH. S.-C.L. acknowledges the support from KIST (2E20200). Experiments at PLS were supported in part by MOST and POSTECH. H.-J.C. thanks to Dr. Young-Ho Lee for his TEM analysis and Dr. Dong-Ryeol Lee and Hyun-Hwi Lee for AXS measurements at beamline 5A1-HFMS of PLS. H.-J.C. also thanks the RAME Center, KICET for the use of their facilities.

Supporting Information Available: Synchrotron X-ray diffraction scans for nanowires, temperature-dependent resistance of typical $Ga_{1-x}Cu_xN$ nanowires, XMCD data from the difference between the Ni $L_{2,3}$ edge XAS spectra for the different spin directions of $Ga_{1-x}Cu_xN$ nanowires for $x = 0.01$ and 0.024 measured at 10 K. This material is available free of charge via the Internet at http://pubs.acs.org.

References

(1) Sarma, S. D. *Nat. Mater.* **2003**, *2*, 292.
(2) Malajovich, I.; Berry, J. J.; Samarth, N.; Awschalom, D. D. *Nature* **2001**, *411*, 770.
(3) Ohno, H. *Science* **1998**, *281*, 951.
(4) Wolf, S. A.; Awschalom, D. D.; Buhrman, R. A.; Daughton, J. M.; von Molnar, S.; Roukes, M. L.; Chtchelkanova, A. Y.; Treger, D. M. *Science* **2001**, *294*, 1488.
(5) Dietl, T.; Ohno, H.; Matsukura, F.; Cibert, J.; Ferrand, D. *Science* **2000**, *287*, 1019.
(6) Lee, J. S.; Lim, J. D.; Khim, Z. G.; Park, Y. D.; Pearton, S. J.; Chu, S. N. G. *J. Appl. Phys.* **2003**, *93*, 4512.
(7) Neal, J. R.; Behan, A. J.; Ibrahim, R. M.; Blythe, H. J.; Ziese, M.; Fox, A. M.; Gehring, G. A. *Phys. Rev. Lett.* **2006**, *96*, 197208.
(8) Matsumoto, Y.; Murakami, M.; Shono, T.; Hasegawa, T.; Fukumura, T.; Kawasaki, M.; Ahmet, P.; Chikyow, T.; Koshihara, S.; Koinuma, H. *Science* **2001**, *291*, 854.
(9) Zaja, M.; Gosk, J.; Granka, E.; Kaminska, M.; Twardowski, A.; Strojek, B.; Szyszko, T.; Podsiadlo, S. *J. Appl. Phys.* **2003**, *93*, 4715.
(10) Kim, J. Y.; Park, J. H.; Park, B. G.; Noh, H. J.; Oh, S. J.; Yang, J. S.; Kim, D. H.; Bu, S. D.; Noh, T. W.; Lin, H. J.; Hsieh, H. H.; Chen, C. T. *Phys. Rev. Lett.* **2003**, *90*, 017401.
(11) Ando, K.; Saito, H.; Jin, Z.; Fukumura, T.; Kawasaki, M.; Matsumoto, Y.; Koinuma, H. *J. Appl. Phys.* **2001**, *89*, 7284.
(12) Thillosen, N.; Sebald, K.; Hardtdegen, H.; Meijers, R.; Calarco, R.; Montanari, S.; Kaluza, N.; Gutowski, J.; Luth, H. *Nano Lett.* **2006**, *6*, 704.
(13) Holleitner, A. W.; Sih, V.; Myers, R. C.; Gossard, A. C.; Awschalom, D. D. *Phys. Rev. Lett.* **2006**, *97*, 036805.
(14) Cui, X. Y.; Delley, B.; Freeman, A. J.; Stampfl, C. *Phys. Rev. Lett.* **2006**, *97*, 016402.
(15) Liao, Z. M.; Li, Y.; Xu, J.; Zhang, J.; Xia, K.; Yu, D. *Nano Lett.* **2006**, *6*, 1087.
(16) Choi, H. J.; Seong, H. K.; Chang, J.; Lee, K. I.; Park, Y. J.; Kim, J. J.; Lee, S. K.; He, R.; Kuykendall, T.; Yang, P. *Adv. Mater.* **2005**, *17*, 1351.
(17) Seong, H. K.; Lee, Y.; Kim, J. Y.; Byeun, Y. K.; Han, K. S.; Park, J. G.; Choi, H. J. *Adv. Mater.* **2006**, *18*, 3019.
(18) Scarpulla, M. A.; Cardozo, B. L.; Farshchi, R.; Hlaing Oo, W. M.; McCluskey, M. D.; Yu, K. M.; Dubon, O. D. *Phys. Rev. Lett.* **2005**, *95*, 207204.
(19) Sasaki, T.; Sonoda, S.; Yamamoto, Y.; Suga, K.; Shimizu, S.; Hori, H. *J. Appl. Phys.* **2002**, *91*, 7911.
(20) The atomic scattering factors are the combination of nonresonant Thomson scattering factor f_0 and anomalous scattering factor Δf composed of real part f' and imaginary part f'' ($\Delta f = f' + i f''$). The depth of cusps at absorption edges depend on the concentration of a specific element in that refection. A concentration of a specific element in the reflection resulted in a cusp at the relevant absorption edge. Absence of a cusp at the related absorption edge indicated the absence of that specific element in the reflection.
(21) Chaboy, J.; Munoz-Paez, A.; Carrera, F.; Merkling, P.; Marcos, E. S. *Phys. Rev. B* **2005**, *71*, 134208.
(22) Finazzi, M.; Ghiringhelli, G.; Tjernberg, O.; Ohresser, Ph.; Brookes, N. B. *Phys. Rev. B* **2000**, *61*, 4629.
(23) van der Laan, G.; Pattrick, R. A. D.; Henderson, C. M. B; Vaughan, D. J. *J. Phys. Chem. Solids* **1992**, *53*, 1185.
(24) Griori, M.; van Acker, J. F.; Czyzyk, M. T.; Fuggle, J. C. *Phys. Rev. B.* **1992**, *45*, 3309.
(25) Buchholz, D. B.; Chang, R. P. H.; Song, J. H.; Ketterson, J. B. *Appl. Phys. Lett.* **2005**, *87*, 082504.
(26) Errico, L. A.; Renteria, M.; Weissmann, M. *Phys. Rev. B* **2005**, *72*, 184425.
(27) Duhalde, S.; Vignolo, M. F.; Golmar, F.; Chiliotte, C.; Rodriguez Torres, C. E.; Errico, L. A.; Cabrera, A. F.; Renteria, M.; Sanchez, F. H.; Weissmann, M. *Phys. Rev. B.* **2005**, *72*, 161313(R).
(28) Shim, J. H.; Hwang, T.; Lee, S.; Park, J. H.; Han, S. J.; Jeong, Y. H. *Appl. Phys. Lett.* **2005**, *86*, 082503.
(29) Park, M. S.; Min, B. I. *Phys. Rev. B* **2003**, *68*, 224436.

NL0716552